Citation: CPT Pharmacometrics Syst. Pharmacol. (2016) 5, 211–221; doi:10.1002/psp4.12075

ORIGINAL ARTICLE

Translational Pharmacokinetic-Pharmacodynamic Modeling and Simulation: Optimizing 5-Fluorouracil Dosing in Children With Pediatric Ependymoma

VM Daryani[1], YT Patel[1], M Tagen[2], DC Turner[3], AM Carcaboso[4], JM Atkinson[5], A Gajjar[6], RJ Gilbertson[7], KD Wright[6] and CF Stewart[1]*

We previously investigated novel therapies for pediatric ependymoma and found 5-fluorouracil (5-FU) i.v. bolus increased survival in a representative mouse model. However, without a quantitative framework to derive clinical dosing recommendations, we devised a translational pharmacokinetic-pharmacodynamic (PK-PD) modeling and simulation approach. Results from our preclinical PK-PD model suggested tumor concentrations exceeded the 1-hour target exposure (*in vitro* IC_{90}), leading to tumor growth delay and increased survival. Using an adult population PK model, we scaled our preclinical PK-PD model to children. To select a 5-FU dosage for our clinical trial in children with ependymoma, we simulated various 5-FU dosages for tumor exposures and tumor growth inhibition, as well as considering tolerability to bolus 5-FU administration. We developed a pediatric population PK model of bolus 5-FU and simulated tumor exposures for our patients. Simulations for tumor concentrations indicated that all patients would be above the 1-hour target exposure for antitumor effect.
CPT Pharmacometrics Syst. Pharmacol. (2016) **5**, 211–221; doi:10.1002/psp4.12075; published online 14 April 2016.

Study Highlights

WHAT IS THE CURRENT KNOWLEDGE ON THE TOPIC? ☑ Although 5-FU is often administered as a continuous infusion, our preclinical studies in pediatric ependymoma showed bolus administration improved survival. However, no bolus pediatric PK data existed to provide dosing recommendations. • WHAT QUESTION DID THIS STUDY ADDRESS? ☑ We utilized a modeling and simulation approach using a preclinical PK-PD model and an adult PK model to recommend initial dosages for our phase I trial and determined the disposition of bolus 5-FU in children with recurrent ependymoma. • WHAT THIS STUDY ADDS TO OUR KNOWLEDGE ☑ The recommended phase II dosage from our phase I trial derived from our translational PK-PD M&S approach was tolerable and the simulated tECF concentrations were above the targeted exposure (*in vitro* IC_{90}). • HOW THIS MIGHT CHANGE CLINICAL PHARMACOLOGY AND THERAPEUTICS ☑ Because ependymomas lack effective chemotherapy, we utilized PK-PD M&S to translate bolus 5-FU to the clinic. This approach is applicable to other settings for translating new or optimizing existing therapies for other diseases to improve drug development.

Pediatric ependymomas are predominantly localized to the posterior fossa with a median age at diagnosis of 6 years old and a 7-year event-free survival nearing 70%.[1] Primary treatment for nonmetastatic disease consists of both surgery and local field radiation. In children <3 years old, chemotherapy has been used to delay radiation-related side effects, including neurocognitive and endocrine deficits.[2] Approximately 33% to 50% of patients relapse because of local failure, distant disease, or a combination, leading to fatal outcomes in 90% of these patients.[3] The median 5-year progression-free survival and overall survival from a recent retrospective study in relapsed patients with ependymoma were 17% and 27.6%, respectively.[3]

Because of the rarity of this disease, clinical evaluation of novel therapies remains challenging. We previously reported on a process for investigating novel therapies for pediatric ependymomas that showed i.v. bolus 5-fluorouracil (5-FU) was efficacious in a mouse model of pediatric ependymoma.[4] A purine antimetabolite, 5-FU, is used to treat several adult malignancies, most notably colorectal cancer. It rapidly enters cells where it is converted to several active metabolites that cause downstream DNA and RNA damage.[5] In pediatric malignancies, 5-FU is usually administered as a continuous infusion for the treatment of adolescent colorectal cancer and nasopharyngeal carcinoma, whereas in smaller clinical trials, i.v. bolus 5-FU has been used to treat recurrent solid tumors.[6–10] Little is known regarding 5-FU pharmacokinetics (PKs) in pediatrics; one study in 31 children with refractory solid tumors reported the mean 5-FU clearance after a 12-hour infusion to be similar to adult estimates.[11]

The clinical use of 5-FU dates back decades, but due to the paucity of pediatric 5-FU PK data, we lacked a rigorous

[1]Department of Pharmaceutical Sciences, St. Jude Children's Research Hospital, Memphis, Tennessee, USA; [2]Genentech, South San Francisco, California, USA; [3]Quantitative Pharmacology and Pharmacometrics, Merck Research Laboratories, Rahway, New Jersey, USA; [4]Preclinical Therapeutics and Drug Delivery Research Program, Hospital Sant Joan de Déu Barcelona, Barcelona, Spain; [5]Department of Pediatrics, Pennsylvania State College of Medicine, Hershey, Pennsylvania, USA; [6]Department of Oncology, St. Jude Children's Research Hospital, Memphis, Tennessee, USA; [7]Cambridge Cancer Centre, Cambridge, UK. *Correspondence: CF Stewart (clinton.stewart@stjude.org)
Received 17 February 2016; accepted 3 March 2016; published online on 14 April 2016. doi:10.1002/psp4.12075

quantitative framework for scaling preclinical findings for use in the clinic. Therefore, we devised a translational modeling and simulation (M&S) approach to determine an initial dosage for bolus 5-FU for a phase I clinical trial in children with recurrent ependymoma.[12] The objectives of this report are to describe our preclinical PK-pharmacodynamic (PD) studies and M&S techniques used to determine the initial bolus 5-FU dosing regimen for a phase I study in pediatric patients with recurrent ependymoma. Additionally, we describe the first population PK analysis for bolus 5-FU in children, which when linked with a preclinical tumor PK model was used to simulate target exposures.

METHODS AND MATERIALS

Preclinical PK and efficacy studies

The preclinical plasma PK, cerebral microdialysis, and efficacy studies used here for preclinical PK-PD model development were published in our previous manuscript[4] or are described in the **Supplementary Material**. Briefly, plasma PK studies of 5-FU were performed in two groups of nontumor bearing mice receiving 5-FU 75 mg/kg i.v. bolus via tail vein injection or subcutaneous continuous infusion over 3 days. Cerebral microdialysis studies were performed in mice bearing pediatric ependymoma receiving 5-FU 75 mg/kg i.v. bolus or 13 mg/kg/hr over 24 hours via subcutaneous infusion. Plasma samples and dialysate fractions were collected at predetermined timepoints after drug administration and analyzed using a validated high-performance liquid chromatography method.[13] For preclinical efficacy studies, mice were randomized to control or treatment groups 7 days after tumor implantation based on their luciferase-mediated bioluminescence signal, a measure of tumor growth. Mice were dosed according to the following schedules: (1) 5-FU 75 mg/kg i.v. bolus weekly for 4 weeks; (2) 5-FU 75 mg/kg subcutaneous infusion over 3 or 5 days every 3 weeks; and (3) 5-FU 37.5 or 75 mg/kg i.v. bolus weekly for 4 weeks.

PK-PD modeling of preclinical data

PK-PD data were analyzed by nonlinear mixed effects modeling using NONMEM 7.3 (ICON Development Solutions, Ellicott City, MD). The interindividual and residual variability were parameterized exponentially and proportionally in the model, respectively. The Akaike information criterion value and inspection of diagnostic plots were used to select between competing models. A visual predictive check was performed by simulating 1,000 concentration time or tumor growth profiles at each dosage. The standard errors of PK model parameter estimates were determined by running covariance steps, whereas confidence intervals of the PD parameter estimates were determined by performing bootstrap analysis consisting of 500 runs.

First, a one or two-compartment model with linear or Michaelis–Menten elimination was tested on all 5-FU plasma concentration-time data. Parameters from the final plasma PK model were fixed and used as inputs to the tumor PK model, which included the 5-FU tumor extracellular fluid concentration (tECF). Several different tumor PK models were tested, including one or two-compartment models with linear or Michaelis–Menten kinetics. Based on the assumption that only free drug crosses the blood-brain barrier, the 5-FU amount in the central compartment (A(1)) was multiplied by the fraction unbound in the differential equations.[14] Because the microdialysate was collected in fractions (30 min/fraction for bolus and 4 h/fraction for infusion), each fraction was modeled as a separate compartment using the MTIME option in NONMEM to code when a new fraction was collected. The microdialysate flow rate, tubing lag time, and the total volume of each fraction were fixed to experimental values. The area under the concentration-time curve profiles were estimated by integrating the predicted concentration-time profiles to a specific time after dosing (t). The tumor to plasma partition coefficient for unbound 5-FU ($K_{pt,uu}$) was estimated as a ratio of unbound tumor to plasma area under concentration values.

Bioluminescence data for each mouse were normalized to the value at day 7 after tumor cell implantation. The tumor growth model, based on a previously described model, contains exponential and linear tumor growth phases, and three transit compartments representing drug-induced cell death.[15] The differential equations representing tumor growth and drug induced cell death are as follows:

$$\frac{dL_1(t)}{dt} = \frac{K_{\exp,m} * L_1(t)}{\left[1+\left(\frac{K_{\exp,m}}{K_{lin,m}} * L_1(t)\right)^{\Psi_m}\right]^{1/\Psi_m}} - K_m * L_1(t)$$

$$\frac{dL_2(t)}{dt} = K_m * L_1(t) - K_{del,m} * L_2(t)$$

$$\frac{dL_3(t)}{dt} = K_{del,m} * L_2(t) - K_{del,m} * L_3(t)$$

$$\frac{dL_4(t)}{dt} = K_{del,m} * L_3(t) - K_{del,m} * L_4(t)$$

$$W(t) = L_1(t) + L_2(t) + L_3(t) + L_4(t)$$

$L_1(t)$ represents proliferating cells within whole tumor; $L_2(t)$, $L_3(t)$, and $L_4(t)$ are tumor growth of cells in transit compartments after drug treatment. $W(t)$ is the fold increase in tumor bioluminescence at any time (t) after 0. $K_{exp,m}$ and $K_{lin,m}$ are the exponential and linear growth rates, respectively; Ψ_m is the constant that related to switching tumor growth from exponential to linear; K_m is the drug inhibitory effect on tumor growth; $K_{del,m}$ is a first order rate constant for the transit compartments. Because the tumor size was normalized to baseline bioluminescence, W(0) was fixed to 1. The inhibitory effect of the drug on tumor growth (K_m) was modeled with a sigmoidal E_{max} equation[15]:

$$K_m = \frac{k_{\max,m} * C_{tECF}^{H_m}}{EC_{50,m}^{H_m} + C_{tECF}^{H_m}}$$

where $k_{max,m}$ is the maximal effect of the drug; $EC_{50,m}$ is the concentration producing half the maximal effect; C_{tECF} is the model predicted 5-FU concentration in the tECF; and H_m is the Hill coefficient.

Scaling of adult PK model and qualification for pediatric patients

To translate our preclinical PK-PD model to the clinic for use in children with ependymoma, an adult 5-FU bolus population PK model was used because of the limited pediatric 5-FU PK information available.[16] Terret *et al.*[16] published a two-compartment plasma PK model with Michaelis–Menten elimination and body surface area (BSA) as a covariate on V_{max}. To account for the wider range of BSA in children, we BSA-normalized the volume of the central compartment (V_1) (**Supplementary Table S1**).[16] We simulated 1,000 pediatric 5-FU concentration time profiles after a 12-hour 5-FU infusion using the scaled-adult model and compared the simulated concentrations to published pediatric data.[11]

Simulation of tumor exposure and tumor growth inhibition

The scaled-adult plasma PK model was linked to the preclinical PK-PD model by fixing the tumor growth and drug effect parameters and changing the plasma fraction unbound (f_u) value from mouse to human. Tumor exposure and tumor growth inhibition were simulated for various 5-FU bolus dosages based on those used in a previous pediatric trial.[9] Dosage levels were assessed for percentage of simulated profiles reaching the targeted exposure (1-hour *in vitro* IC_{90}) and for tumor growth inhibition. The simulated results were used along with a knowledge of the tolerability to i.v. bolus 5-FU to determine a recommended phase I dosage for use in a clinical trial to treat children with recurrent ependymoma.

Pediatric population PK study

Patient population and PK sampling strategy. Details regarding eligibility, study design, and PK sampling strategy are described in a previous publication.[17]

Population PK modeling

In total, 570 concentration-timepoints were utilized for the development of the population PK model. Various compartmental structural models were tested to describe 5-FU plasma concentrations including one, two, and three-compartment models with linear and/or saturable elimination. Interindividual (between subject) and interoccasion (within-subject) variability were explored assuming a log-normal distribution of the parameters. Treatment occasions were defined as a group of concentration-time data after a single 5-FU bolus administration. A combined additive and proportional error model was chosen to explain the residual variability in observed concentrations.

BSA was incorporated in the model parameterization *a priori* and the following covariates were tested and evaluated graphically to explain the interindividual variability of the population PK model: baseline age, race, actual body weight, sex, albumin, alanine aminotransferase, aspartate aminotransferase, estimated creatinine clearance,[18,19] total protein, and total bilirubin. A covariate was considered significant in this analysis if the addition to the model reduced the -2 log-likelihood by 3.84 units or greater ($P < 0.05$) based on the χ^2 goodness-of-fit test and a difference of one degree of freedom.

Approaches for analyzing PK data below the limit of quantitation (BLQ) were explored and parameter estimation was performed using the LAPLACIAN and Monte Carlo Importance Sampling estimation method with the covariance step in NONMEM 7.3.[20] The predictive performance of the model was evaluated by visual predictive check simulating 1,000 versions of the original data using the final model parameters.

Pediatric tECF simulations

We linked the pediatric 5-FU population plasma PK model to the preclinical tECF PK model and simulated individual tECF concentration-time profiles using individual *post hoc* parameter estimates to estimate tECF exposures in our patient population. We estimated the percentage of patients reaching the targeted exposure (1-hour *in vitro* IC_{90}) to evaluate the success of our translational approach.

RESULTS

Plasma protein binding

The 5-FU protein binding in mouse plasma was determined using equilibrium dialysis at concentrations of 10 and 100 μM. As shown in **Supplementary Figure S1**, equilibrium between the donor and receptor chamber was reached within 8 hours. Mean 5-FU fraction unbound in mouse plasma was 0.37 ± 0.05. No significant difference was observed in fraction unbound at equilibrium between the two 5-FU concentrations, suggesting concentration-independent binding of 5-FU in mouse plasma within this range of concentrations.

Development of preclinical PK-PD model

We first developed a preclinical plasma PK model representing the 5-FU total plasma concentration-time data. Among the models tested, a two-compartment model with Michaelis–Menten elimination from the central compartment (**Figure 1, Step 1a**) best represented the 5-FU plasma profiles (**Figure 2a–c**). The 5-FU showed nonlinear, saturable elimination in mouse plasma with a mean $\pm$ SD maximum plasma concentration (C_{max}) of 536 ± 162 μM after a 75 mg/kg i.v. bolus dose, $\sim$4 times higher than the estimated mean $\pm$ SD $K_{m,plasma}$, 125 ± 22 μM. The mean $\pm$ SD 5-FU plasma steady-state concentration observed after a 1-day or 3-day continuous infusion was 7.11 ± 2.64 μM and 0.43 ± 0.18 μM, $\sim$17 and 300 times lower than the estimated $K_{m,plasma}$, respectively. This nonlinear PK produced higher plasma exposures (area under the curve) at the same dosages after i.v. bolus administration compared to the 3-day or 5-day infusion (**Supplementary Figure S2**).

Next, we developed a PK model representing 5-FU unbound tECF concentration-time data, conditioned on the given plasma PK model. To avoid over-parameterization, plasma PK parameters were fixed to previously estimated values. The volume of tECF compartment (V_3) was fixed to 0.001 L/kg based on published data and assuming tumor weight to be 15% of the mouse brain.[21,22] A two-compartment model with Michaelis–Menten elimination from the tECF compartment best described the tECF concentration-time data (**Figure 2d,e**). The tECF compartment was linked to the plasma compartment using rate constants (K_{13} and K_{31}). The final plasma and tECF PK parameter estimates are listed in **Table 1**. Based on prior *in vitro* assays with ependymoma cell

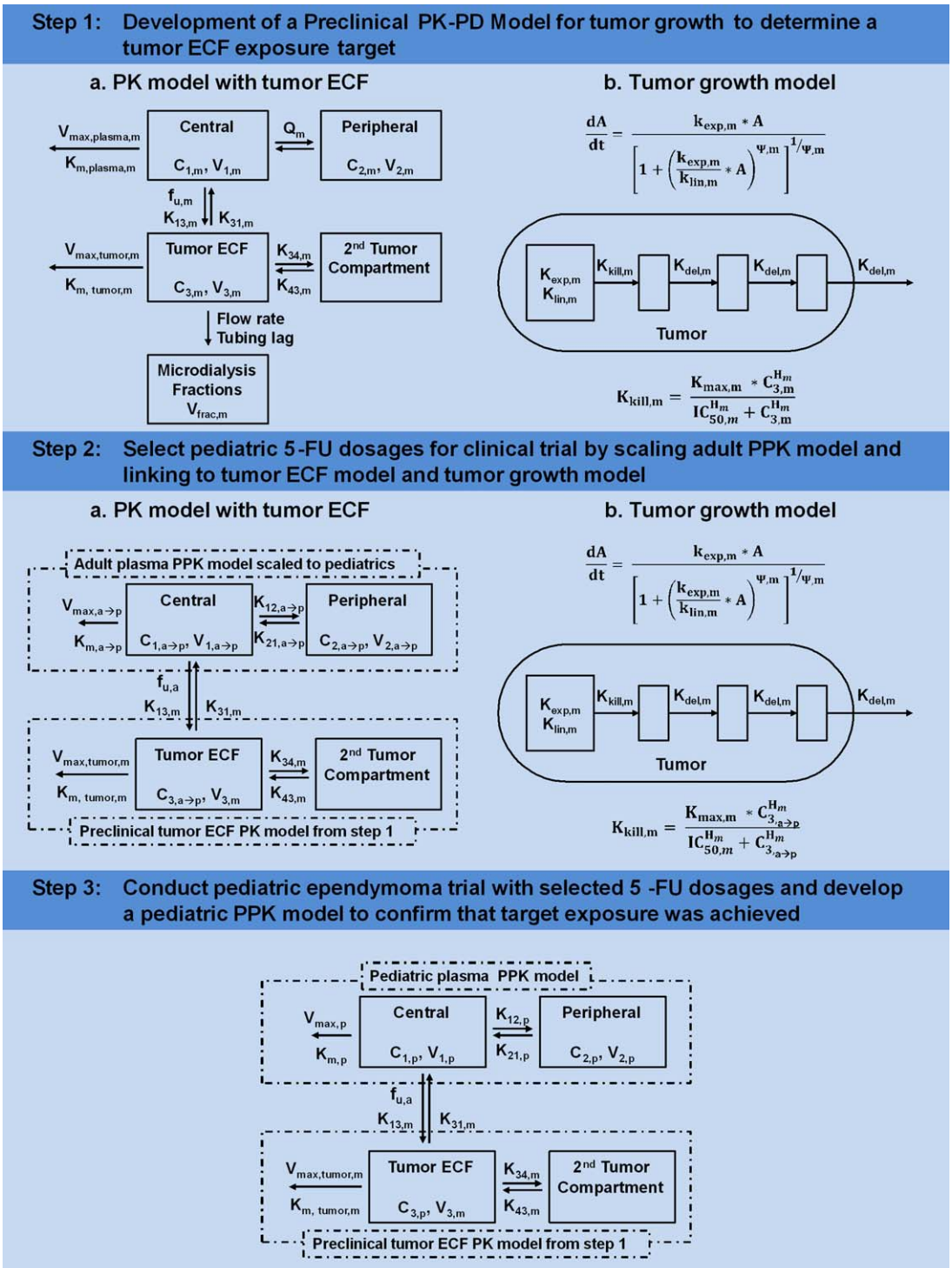

Figure 1 A workflow diagram detailing the preclinical and clinical studies discussed in this article. PPK, population pharmacokinetics; C defines concentration in the corresponding compartment; subscript m defines mouse; subscript "a" defines adult; subscript "p" defines pediatric; subscript "a → p" defines scaled-adult parameter; the remainder of the parameters are defined in **Table 1**.

lines, 7.1 μM was the extracellular IC_{90} for 5-FU induced cell death after a 1-hour incubation.[4] Therefore, 7.1 μM was used as our target exposure for tECF. The 5-FU i.v. bolus tECF concentrations were above this target exposure for ~1 hour, and tECF concentrations after a continuous infusion were at least sevenfold lower.[4]

Last, we developed a PD model representing ependymoma tumor growth in the control and 5-FU-treated CD1

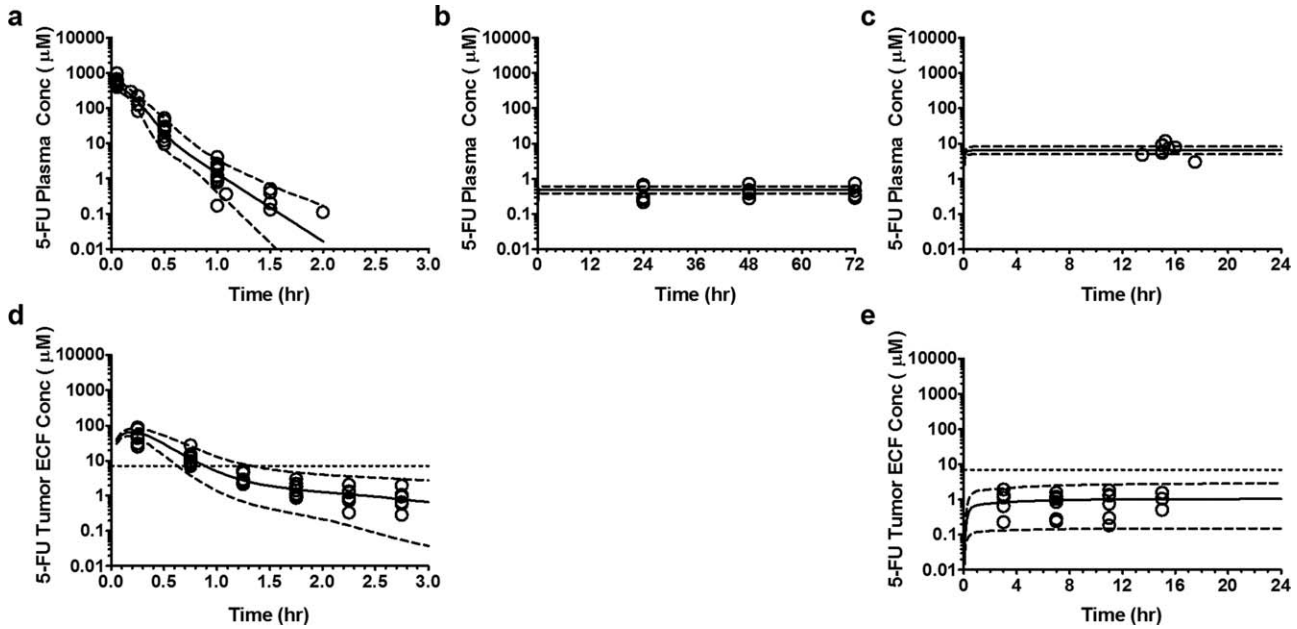

Figure 2 Visual predictive check of preclinical pharmacokinetic model representing plasma and tumor extracellular fluid concentration (tECF) disposition of 5-fluorouracil (5-FU) in ependymoma bearing mice. (**a**, **b**, and **c**) Plasma concentration-time profile of 5-FU at dosage of 75 mg/kg given as i.v. bolus injection, 75 mg/kg given as 3-day infusion, and 13 mg/kg/hr infusion over 24 hours, respectively, plotted on semi-log scale. (**d** and **e**) The tECF concentration-time profile of 5-FU at dosage of 75 mg/kg given as i.v. bolus injection and 13 mg/kg/hr infusion over 24 hours, respectively, plotted on semi-log scale. (Open circle represents observed plasma or tECF concentration; solid line represents the median (50th percentile) of model predicted individual concentrations; dashed line represents the 5th and 95th percentile of model predicted individual plasma concentrations.) **Supplementary Figure 4** shows this figure in the linear scale.

nude mice, conditioned on the plasma-tECF PK model. The 5-FU efficacy studies were performed in three different experimental cohorts with treatment(s) and control groups. During experiment one, mice received 5-FU 75 mg/kg i.v. bolus every week for 4 weeks or no treatment. In experiment two, mice received 5-FU 75 mg/kg subcutaneous infusion over 3 or 5 days every 3 weeks or no treatment. Experiment three compared mice receiving 5-FU 37.5 or 75 mg/kg i.v. bolus every week for 4 weeks. As shown in **Figure 3a–c**, tumor growth data in the control groups (top panels) were best described by exponential and linear growth phases, whereas tumor inhibition by 5-FU was best described by sigmoidal E_{max} model (middle and bottom panels). Because the tumor growth rate in control animals from experiment one was different compared with experiments two and three, the exponential tumor growth term (K_{exp}) was allowed to vary for experiment one and a linear covariate effect was applied to K_{exp1} for experiments two and three using the following structure:

$$TVK_{\exp} = \theta_{K_{\exp 1}} \text{ if experiment one}$$

$$TVK_{\exp} = \theta_{K_{\exp 1}} + \theta_{K_{\exp 2/3}} \text{ if experiments two and three}$$

$$K_{\exp} = TVK_{\exp} * e^{\eta_{K\exp}}$$

The final PD model parameters are provided in **Table 1**. The *in vivo* tECF concentration producing half maximum tumor inhibitory effect (IC_{50}, 2.12 μM) estimated using our PK-PD model was within twofold of our 1-hour *in vitro* IC_{50} (3.5 μM).[4] The 5-FU i.v. bolus resulted in significant tumor growth suppression and subsequent increase in overall survival, whereas 5-FU continuous infusion failed to exhibit tumor suppression, resulting in no difference in survival compared to the control mice.[4] This is consistent with our plasma-tumor PK model that showed 5-FU i.v. bolus achieved tECF concentrations above the target exposure (**Figure 2d**), whereas 5-FU continuous infusion did not (**Figure 2e**). This supports using 5-FU i.v. bolus in children with ependymoma. However, without published pediatric PK data to support dosing recommendations, we decided to utilize our preclinical PK-PD model with available adult 5-FU PK data to establish dosages for our clinical trial.

Model-based determination of efficacious clinical dosage

Scaling of adult 5-FU plasma PK model for pediatrics. To apply our preclinical PK-PD model to pediatric patients, we first scaled an adult plasma two-compartment population PK model with Michaelis–Menten elimination.[16] The scaled-adult model was qualified by performing Monte Carlo simulations of 1,000 pediatric patients and comparing the simulated steady-state concentrations to PK data from a pediatric 5-FU continuous infusion (80 mg/m^2/h infusion over 12 hours).[11] The simulated profiles had a mean steady-state concentration of 4.1 μM, within twofold of the pediatric mean steady-state concentration (6.7 μM), supporting further use of the adult scaled-model for pediatric dosage simulations.

Table 1 Final parameter estimates for preclinical PK-PD model fitted to mouse 5-FU plasma and tECF disposition and efficacy studies

Parameters	Unit	Estimate ± SE	IIV (% CV)
Plasma PK study			
Maximum plasma 5-FU elimination rate ($V_{max,plasma,m}$)	μmol/hr/kg	2040 ± 239	12.2
Michaelis–Menten constant for plasma 5-FU elimination ($K_{m,plasma,m}$)	μM	125 ± 22	NE
Volume of central compartment ($V_{1,m}$)	L/kg	0.962 ± 0.691	22.1
Intercompartmental clearance (Q_m)	L/hr/kg	1.67 ± 1.03	31.1
Volume of peripheral compartment ($V_{2,m}$)	L/kg	0.332 ± 0.50	NE
Residual variability for 5-FU plasma concentrations ($\sigma_{plasma,\ prop}$)	% CV	30.7	
Tumor microdialysis study			
Rate constant for 5-FU movement from plasma to tECF ($K_{13,m}$)	1/hr	0.0043 ± 0.001	7.8
Rate constant for 5-FU movement from tECF to plasma ($K_{31,m}$)	1/hr	3.24 ± 0.58	26.1
5-FU fraction unbound in mouse plasma ($f_{u,m}$)		0.37 FIX	NE
Volume of tECF compartment ($V_{3,m}$)	L/hr	0.001 FIX	NE
Rate parameter for intratumoral 5-FU disposition ($K_{34,m}$)	1/hr	1.82 ± 0.30	NE
Rate parameter for intratumoral 5-FU disposition ($K_{43,m}$)	1/hr	0.334 ± 0.077	NE
Maximum tumor 5-FU elimination rate ($V_{max,tumor,m}$)	μmol/hr/kg	0.0063 ± 0.004	NE
Michaelis–Menten constant for tumor 5-FU elimination ($K_{m,tumor,m}$)	μM	0.012 ± 0.023	NE
Residual variability for 5-FU plasma concentrations ($\sigma_{plasma,\ prop}$)	% CV	35.9	
Residual variability for 5-FU tumor concentrations ($\sigma_{tECF,\ prop}$)	% CV	27.9	
Efficacy study			
Exponential tumor growth parameter ($\theta_{K_{exp,m,\ 1}}$) for experiment one	1/hr	0.158 (0.079–0.337)[a]	40.6
Linear covariate effect on $\theta_{K_{exp,m,1}}$ for experiments two and three ($\theta_{K_{exp,m,\ 2/3}}$)	1/hr	0.102 (0.031–0.287)[a]	
Linear tumor growth parameter ($K_{lin,m}$)	1/hr	214,000 (66,700–1,480,000)[a]	NE
Constant related to switching tumor growth from exponential to linear (Ψ_m)		0.0936 (0.085–0.104)[a]	NE
Maximum 5-FU tumor inhibitory effect ($K_{max,m}$)	1/hr	0.658 (0.316–1.134)[a]	NE
5-FU tECF concentration producing half the maximum tumor inhibitory effect ($IC_{50,m}$)	μM	2.12 (0.28–5.84)[a]	30.4
Hill coefficient (H_m)		1.22 (0.64–1.89)[a]	NE
Rate constant transit tumor compartment ($K_{del,m}$)	1/hr	0.946 (0.124–1.950)[a]	NE
Residual variability for tumor growth ($\sigma_{efficacy,\ prop}$)	% CV	37.0	

5-FU, 5-fluorouracil; CV, coefficient of variation; FIX, value fixed during estimation; IIV, interindividual variability; NE, not estimated; PK-PD, pharmacokinetic-pharmacodynamic; tECF, tumor extracellular fluid concentration.
[a]Values represent 2.5th and 97.5th percentile of bootstrap-derived parameter estimates.

Application of scaled-adult model to determine pediatric dosage. By linking the scaled-adult plasma PK model with the preclinical PK-PD model, we compared predicted tECF concentrations to the 1-hour IC_{90} (7.1 μM) and investigated tumor growth inhibition to determine a potentially efficacious 5-FU bolus dosage in children with brain tumors. To accurately estimate unbound 5-FU tumor concentrations, we used published data showing the 5-FU plasma fraction unbound was 0.9.[23] The tECF simulations showed 68%, 90%, and 99% of subjects would have tECF concentrations above the target exposure (7.1 μM) for at least 1-hour at 400, 500, and 650 mg/m^2, respectively (**Figure 4a–c)**. Combined with our simulations for tumor growth inhibition (**Figure 4d–f**), 500 and 650 mg/m^2 dosages were suggested to be highly efficacious. Based on the reported tolerability of 5-FU bolus in pediatrics, we recommended 500 mg/m^2 as the starting dosage with 400 mg/m^2 as dosage level zero (dose deescalation) and 650 mg/m^2 as dose level two (dose escalation) for our clinical trial of single-agent 5-FU in children with recurrent/refractory ependymoma.

Population PK modeling of pediatric data and simulation of tumor exposures

Study population. The pediatric phase I study consisted of 26 children and young adults with recurrent/refractory ependymoma. The patient cohort had a median age of 7.1 years old with 18 girls (69.2%) and 8 boys (30.8%), and the majority were white (73.1%). The PK data were available for patients receiving 400, 500, and 650 mg/m^2 dosage of 5-FU. The baseline demographics are shown in **Supplementary Table S2**.

Model development. We explored a one or two-compartment model structure with linear or saturable elimination and various model parameterizations.[24] Approximately 40% of samples assayed were found to be BLQ, 15 μM, and approaches for modeling PK data BLQ were explored.[20]

A two-compartment structural model best fit the 5-FU plasma concentration-time data, which followed a bi-exponential decay. The final model had first-order elimination from the central compartment using a BSA normalized dosage. The M3 method was used for BLQ data, leading to improved accuracy in parameter estimation (lower relative standard error %), a lower Akaike information criterion, and improved model diagnostics (visual predictive checks). The model was parameterized in terms of total systemic clearance (CL_t), volume of the central compartment (V_c), intercompartmental clearance (Q), and volume of the peripheral compartment (V_p). The individual predicted vs. observed concentrations were equally distributed above and below the line of unity and individual weighted residuals vs. predicted

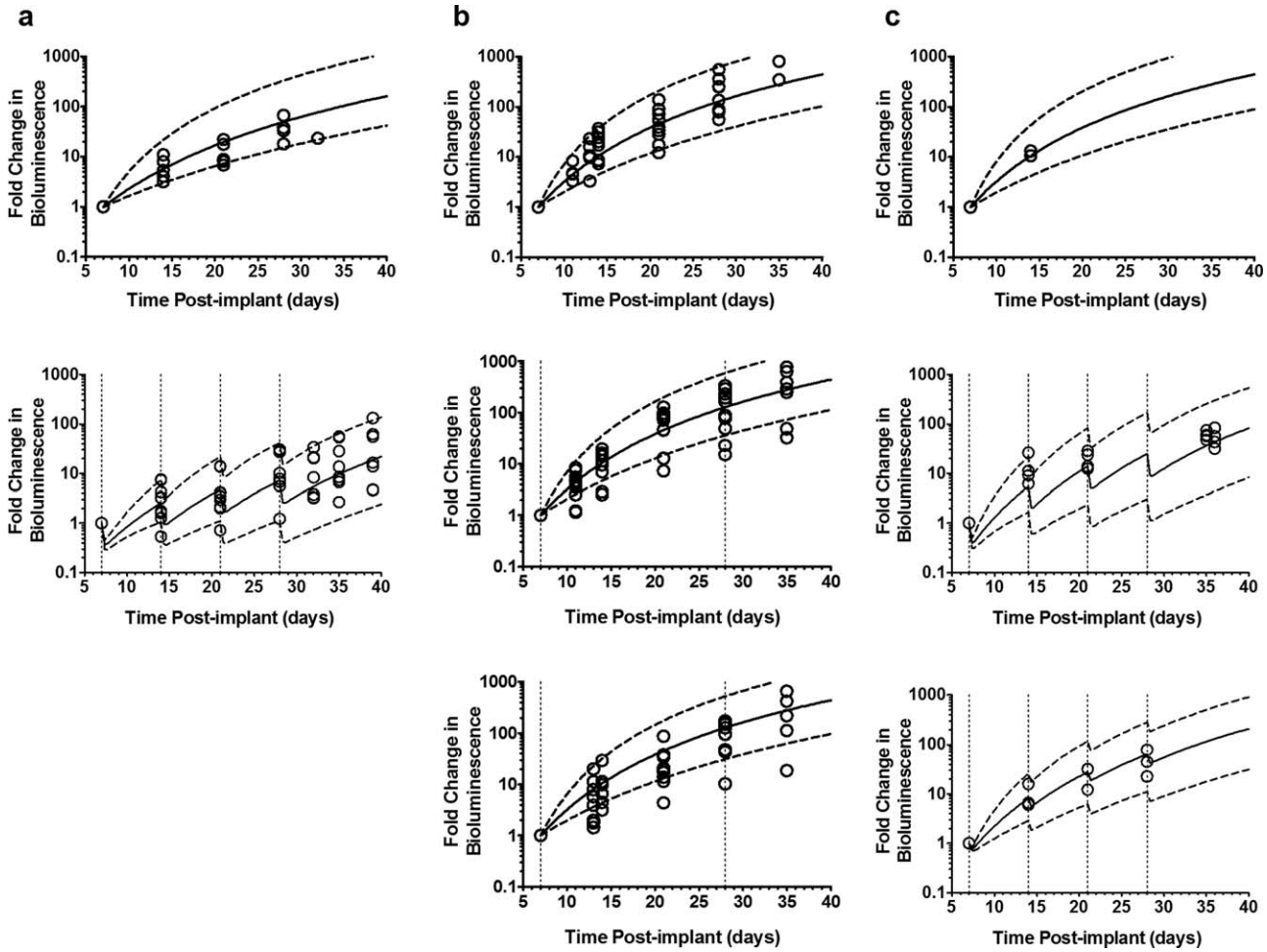

Figure 3 Visual predictive check of preclinical pharmacodynamics model representing tumor growth in control and treated groups in ependymoma bearing mice. (**a**) Experiment one in which mice were either not treated (top) or treated with 75 mg/kg i.v. bolus 5-fluorouracil (5-FU) once every week (bottom); (**b**) represents experiment two in which mice were either not treated (top) or treated with 75 mg/kg 5-FU infusion over 3 (middle) or 5 days (bottom) once every 21 days; (**c**) represents experiment three in which mice were either not treated (top) or treated with 75 (middle) or 37.5 (bottom) mg/kg i.v. bolus 5-FU once every week. (Open circle represents observed fold increase in bioluminescence; solid line represents the median (50th percentile) of model predicted individual fold increase in bioluminescence; dashed line represents the 5th and 95th percentile of model predicted individual fold increase in bioluminescence; vertical dotted lines indicate 5-FU dosing.)

concentrations were symmetrically distributed about zero, suggesting an adequate structural model (**Figure 5**). The parameter estimates for the final structural model are presented in **Table 2**. Moderate interindividual variability (28.8% for CL_t and 26.6% for V_c) and low interoccasion variability (13.0% for CL_t) were estimated for 5-FU parameters. A visual predictive check (**Figure 5** and **Supplementary Figure S5**) supports the structural model is appropriate for 5-FU bolus PK data from our pediatric population.

The effects of baseline patient demographics and laboratory values on each parameter were assessed graphically. Given the model parameterization of BSA as a covariate *a priori*, no other definitive relationship was noted between 5-FU PK parameters and other covariates explored.

Simulation of tECF concentrations using the pediatric population PK model. To estimate tECF concentrations in our patients, we linked the pediatric 5-FU population PK model to the preclinical tECF PK model and used individual *post hoc* parameter estimates to simulate individual tECF concentration-time profiles. All 26 patients on each occasion achieved tECF concentrations at or above the target exposure at 1 hour with a median (range) concentration at 1 hour of 182.5 μM (51.8–754.1 μM).

DISCUSSION

Ependymomas are one of the most challenging malignancies to treat in pediatric oncology because of extensive biological heterogeneity and lack of effective chemotherapeutic agents to date. We previously reported on the preclinical efficacy of 5-FU in a subtype of ependymoma.[4] Herein, we discussed the M&S approach used to translate the results of our 5-FU *in vitro* and *in vivo* studies in ependymoma to patients. Using our preclinical PK-PD model with available

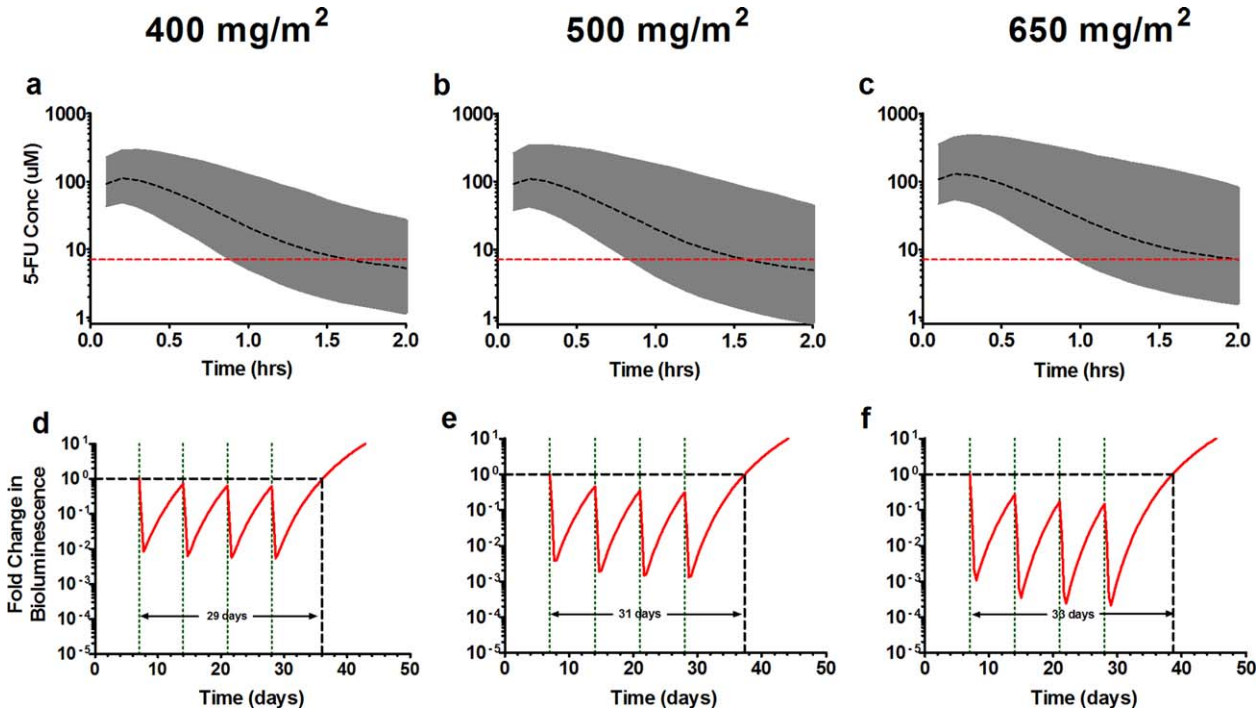

Figure 4 Simulation of the combined scaled-adult plasma pharmacokinetic (PK) model and preclinical PK-pharmacodynamic (PD) model for pediatric dosing regimens. The top row represents predicted tumor extracellular fluid concentration (tECF) concentration-time profiles and the bottom predicted tumor growth profiles. Top: Shown in the black dashed line is the median (50th) percentile, the gray shaded region represents the 95% confidence interval of the Monte Carlo model simulations, and the red horizontal dashed line is the 1-hour *in vitro* IC_{90} (7.1μM). Bottom: The red line represents fold change in bioluminescence in 5-fluorouracil (5-FU) treated tumors. The black horizontal dashed line represents tumor condition at baseline and serves as a reference to calculate tumor growth delay. The green vertical dotted lines represent 5-FU dosing.

data from the literature, we defined a dosage regimen for bolus 5-FU in children with ependymoma. Last, we reported the first population PK model for bolus 5-FU in children and simulated the expected target exposures in our patients.

For the preclinical 5-FU PK-PD model of pediatric ependymoma, we performed PK studies in plasma and tECF, and PD studies measuring tumor growth by luciferase mediated bioluminescence. The 5-FU plasma and tumor concentrations exhibited a bi-exponential elimination and dose-dependent clearance, best described using a two-compartment model with Michaelis–Menten elimination (**Figure 1, Step 1**). The delay in tumor growth between 5-FU treated and control mice was estimated using the PK-PD model (**Supplementary Figure S3**). Mice receiving 75 mg/kg 5-FU i.v. bolus had tumor growth delayed by 16–19 days compared with controls, similar to the 14-day increase in overall survival observed previously (**Supplementary Figure S3a,c**).[4] We acknowledge that bioluminescence has limitations for monitoring tumor growth and may not be applicable across all tumor models[25–28]; however, we found good correlation between survival and tumor growth delay measured using bioluminescence.

To scale the preclinical PK-PD model for use in children with ependymomas, we chose a two-compartment Michaelis–Menten saturable elimination model commonly used to describe the plasma PKs of bolus 5-FU in adults.[16,24,29,30] The adult model was previously validated on external datasets with different dosages and schedules of 5-FU bolus and continuous infusion. The model was qualified on available pediatric data and linked to the tECF PK model and the tumor growth inhibition PD model. After simulating bolus 5-FU dosages for tECF exposure (**Figure 4a–c**), tumor growth inhibition (**Figure 4d–f**), and incorporating knowledge of 5-FU bolus tolerability, we selected 500 mg/m^2 as the phase I dosage for our clinical trial in ependymoma.[9] Using PK data from our phase I trial, we first described 5-FU disposition with a saturable elimination model. However, the two-compartment linear model had comparable model diagnostics and a lower Akaike information criterion (2,439 vs. 2,729).

The 5-FU clearance for this trial was linear across dosages and lower (16.6 L/h/m^2) than previously reported values. Di Paolo *et al.*[31] evaluated the PK of i.v. bolus 5-FU (370 mg/m^2) in patients with colorectal cancer and reported an overall clearance of 51.5 L/h/m^2. Bocci *et al.*[32] investigated the clinical PK of 5-FU and its metabolite in 20 patients with colorectal cancer receiving two different bolus doses (250 and 370 mg/m^2). They found a lower clearance, 25.4 L/h/m^2, in patients receiving 370 mg/m^2 and a higher clearance, 54.6 L/h/m^2, in the same patients receiving a "test" dose of 250 mg/m^2 with the difference attributed to the saturable elimination of 5-FU. Other 5-FU bolus PK models include saturable elimination processes with an approximate V_{max} and K_m of 1,450 mg/h (11,150 μmol/h)

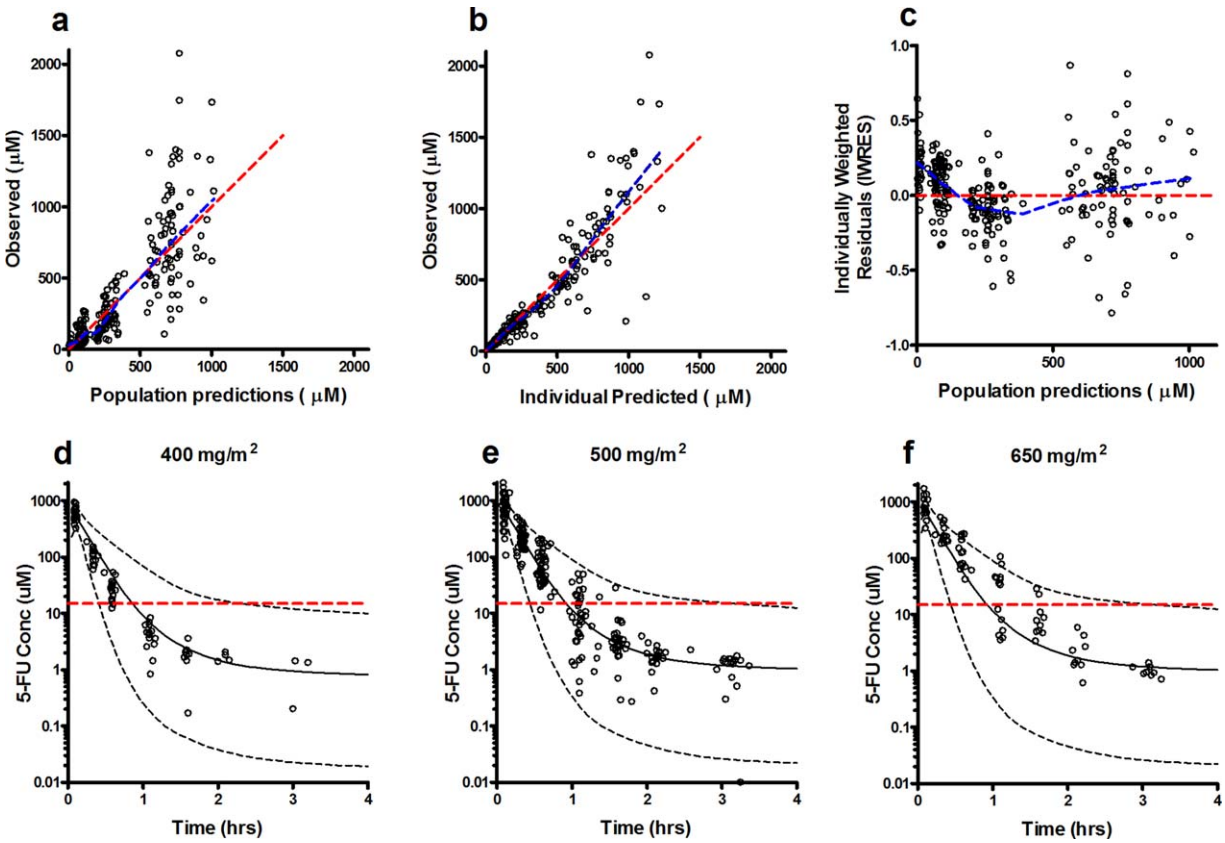

Figure 5 Goodness-of-fit plots for the population pharmacokinetic model of bolus 5-fluorouracil (5-FU) in pediatric patients. The 5-FU observed vs. population (**a**) and individual (**b**) predicted concentrations. Individually weighted residual vs. population predicted concentrations (**c**). (Open circle represents individual values; red dashed line represents the line of identity or a horizontal line at y = 0; purple dashed line represents local regression line (LOWESS)). Visual predictive check for pediatric patients receiving 400 (**d**), 500 (**e**), or 650 (**f**) mg/m^2 5-FU i.v. bolus. (Open circle represents observed individual plasma concentrations; solid line represents the median (50th percentile) of model predicted individual concentrations; dashed lines represent the 5th and 95th percentile of model predicted individual concentrations; the red horizontal dashed line is the lower limit of quantitation.)

and 5 mg/L (40 μM), respectively.[16,29,30] The maximum 5-FU concentrations observed in our phase I study are $\geq$1,000 μM, 50-fold greater than the adult K_m values, which suggests that 5-FU is likely in the concentration range where elimination processes are saturated, resulting in a lower overall clearance (16.6 L/h/m^2). Thus, the high maximum 5-FU plasma concentrations observed relative to the assay BLQ, and the fact that the study was not designed to assess the nonlinearity of 5-FU in children, prevented us from accurately estimating V_{max} and K_m for the Michaelis–Menten model.

In our 5-FU population PK analysis, BSA was a covariate *a priori* on clearance and volume, and no other relationships significantly explained the variability in the PK parameters. The use of adult parameter estimates as priors in the model did not improve model performance. A two-compartment, first order elimination from the central compartment evaluated using the M3 method was an appropriate model for the data.

Approximately 40% of the 5-FU data were BLQ with the majority of these data located in the terminal elimination phase. However, censoring these data would increase the

Table 2 Final pediatric population pharmacokinetic parameter estimates

Parameters	Unit	Estimate ± SE	IIV (% CV)	IOV
Systemic clearance (CL_p)	L/hr/m^2	16.6 ± 1.2	28.8	13.0
Volume of central compartment ($V_{1,p}$)	L/m^2	4.2 ± 0.3	26.6	NE
Intercompartmental clearance (Q_p)	L/hr/m^2	1.6 ± 0.7	80.1	NE
Volume of peripheral compartment ($V_{2,p}$)	L/m^2	20.1 ± 8.6	93.9	NE
Residual variability				
Proportional		0.51 ± 0.04		
Additive		1.98 ± 1.5		

CV, coefficient of variation; IIV, interindividual variability; IOV, interoccasion variability; NE, not estimated.

likelihood for bias in parameter estimates; thus, we investigated methods to handle BLQ data, particularly the M3 method.[20,33] Studies over the past decade describe the M3 method as a reliable approach for data BLQ[20,33–35] and, recently, Keizer *et al*.[36] indicated the least bias may be present by including all BLQ data without incorporating any likelihood-based approaches. The M3 approach resulted in an increased precision in parameter estimation and improvement in model diagnostics.

Given the high rate of drug failures, it is important to perform preclinical experiments in representative tumor models and incorporate clinically relevant dosages/schedules to increase the translation of preclinical research. The translational PK-PD M&S described above is an approach that should serve as a template for drug development in all therapeutic areas, especially rare diseases where the need for promising therapies is high and few patients are available for clinical trials. The results of our preclinical PK-PD M&S confirm our dosage selection for bolus 5-FU and indicate our translational approach achieved the required target exposure for antitumor effect in this phase I trial of recurrent/refractory ependymoma.

Acknowledgments. We are grateful to the staff of Akaike information criterion and ARC at St. Jude Children's Research Hospital for their technical assistance in our work. We are also grateful to Kristen Haddock and K. Elaine Harstead for the bioanalysis of clinical 5-FU samples.

Grants and Financial Support. This work was supported by the Collaborative Ependymoma Research Network (CERN), United States National Institutes of Health Cancer Center Support (CORE) Grant P30 CA21765, and by the American Lebanese Syrian Associated Charities (ALSAC).

Disclosure. The authors have no conflicts of interest to report.

Author Contributions. V.M.D., Y.T.P., M.T., D.C.T., A.M.C., J.M.A., A.G., R.J.G., K.D.W., and C.F.S. wrote the manuscript. M.T., A.M.C., J.M.A., A.G., R.J.G., K.D.W., and C.F.S. designed the research. V.M.D., Y.T.P., M.T., D.C.T., A.M.C., J.M.A., A.G., R.J.G., K.D.W., and C.F.S. performed the research. V.M.D., Y.T.P., M.T., D.C.T., A.M.C., J.M.A., A.G., R.J.G., K.D.W., and C.F.S. analyzed the data. V.M.D. and Y.T.P contributed equally to this work. K.D.W and C.F.S. are co-senior authors of this work.

1. Taylor, M.D. *et al*. Radial glia cells are candidate stem cells of ependymoma. *Cancer Cell* **8**, 323–335 (2005).
2. Grundy, R.G. *et al*. Primary postoperative chemotherapy without radiotherapy for intracranial ependymoma in children: the UKCCSG/SIOP prospective study. *Lancet Oncol.* **8**, 696–705 (2007).
3. Zacharoulis, S., Ashley, S., Moreno, L., Gentet, J.C., Massimino, M. & Frappaz, D. Treatment and outcome of children with relapsed ependymoma: a multi-institutional retrospective analysis. *Childs Nerv. Syst.* **26**, 905–911 (2010).
4. Atkinson, J.M. *et al*. An integrated in vitro and in vivo high-throughput screen identifies treatment leads for ependymoma. *Cancer Cell* **20**, 384–399 (2011).
5. Longley, D.B., Harkin, D.P. & Johnston, P.G. 5-fluorouracil: mechanisms of action and clinical strategies. *Nat. Rev. Cancer* **3**, 330–338 (2003).
6. Hill, D.A. *et al*. Colorectal carcinoma in childhood and adolescence: a clinicopathologic review. *J. Clin. Oncol.* **25**, 5808–5814 (2007).
7. Katzenstein, H.M. *et al*. Hepatocellular carcinoma in children and adolescents: results from the Pediatric Oncology Group and the Children's Cancer Group intergroup study. *J. Clin. Oncol.* **20**, 2789–2797 (2002).
8. Ortega, J.A. *et al*. Randomized comparison of cisplatin/vincristine/fluorouracil and cisplatin/continuous infusion doxorubicin for treatment of pediatric hepatoblastoma: a report from the Children's Cancer Group and the Pediatric Oncology Group. *J. Clin. Oncol.* **18**, 2665–2675 (2000).
9. Patel, R. *et al*. Pharmacology and phase I trial of high-dose oral leucovorin plus 5-fluorouracil in children with refractory cancer: a report from the Children's Cancer Study Group. *Cancer Res.* **51**, 4871–4875 (1991).
10. Pratt, C.B. *et al*. Phase II study of 5-fluorouracil/leucovorin for pediatric patients with malignant solid tumors. *Cancer* **74**, 2593–2598 (1994).
11. Balis, F.M. *et al*. Phase II trial of sequential methotrexate and 5-fluorouracil with leucovorin in children with sarcomas. *Invest. New Drugs* **8**, 181–182 (1990).
12. Stroh, M., Duda, D.G., Takimoto, C.H., Yamazaki, S. & Vicini, P. Translation of anticancer efficacy from nonclinical models to the clinic. *CPT Pharmacometrics Syst. Pharmacol.* **3**, e128 (2014).
13. Alsarra, I.A. & Alarifi, M.N. Validated liquid chromatographic determination of 5-fluorouracil in human plasma. *J. Chromatogr. B Analyt. Technol. Biomed. Life Sci.* **804**, 435–439 (2004).
14. Di, L., Rong, H. & Feng, B. Demystifying brain penetration in central nervous system drug discovery. *Miniperspective. J. Med. Chem.* **56**, 2–12 (2013).
15. Simeoni, M. *et al*. Predictive pharmacokinetic-pharmacodynamic modeling of tumor growth kinetics in xenograft models after administration of anticancer agents. *Cancer Res.* **64**, 1094–1101 (2004).
16. Terret, C. *et al*. Dose and time dependencies of 5-fluorouracil pharmacokinetics. *Clin. Pharmacol. Ther.* **68**, 270–279 (2000).
17. Wright, K.D. *et al*. Phase I study of 5-fluorouracil in children and young adults with recurrent ependymoma. *Neuro. Oncol.* **17**, 1620–1627 (2015).
18. Brandt, J.R., Wong, C.S., Hanrahan, J.D., Qualls, C., McAfee, N. & Watkins, S.L. Estimating absolute glomerular filtration rate in children. *Pediatr. Nephrol.* **21**, 1865–1872 (2006).
19. Schwartz, G.J. *et al*. New equations to estimate GFR in children with CKD. *J. Am. Soc. Nephrol.* **20**, 629–637 (2009).
20. Beal, S.L. Ways to fit a PK model with some data below the quantification limit. *J. Pharmacokinet. Pharmacodyn.* **28**, 481–504 (2001).
21. Brown, R.P., Delp, M.D., Lindstedt, S.L., Rhomberg, L.R. & Beliles, R.P. Physiological parameter values for physiologically based pharmacokinetic models. *Toxicol. Ind. Health* **13**, 407–484 (1997).
22. Hofstein, R., Hesse, G. & Shashoua, V.E. Proteins of the extracellular fluid of mouse brain: extraction and partial characterization. *J. Neurochem.* **40**, 1448–1455 (1983).
23. Czejka, M. & Schüller, J. The binding of 5-fluorouracil to serum protein fractions, erythrocytes and ghosts under in vitro conditions [in German]. *Arch. Pharm. (Weinheim)* **325**, 69–71 (1992).
24. van Kuilenburg, A.B. & Maring, J.G. Evaluation of 5-fluorouracil pharmacokinetic models and therapeutic drug monitoring in cancer patients. *Pharmacogenomics* **14**, 799–811 (2013).
25. Jost, S.C., Collins, L., Travers, S., Piwnica–Worms, D. & Garbow, J.R. Measuring brain tumor growth: combined bioluminescence imaging-magnetic resonance imaging strategy. *Mol. Imaging* **8**, 245–253 (2009).
26. Czupryna, J. & Tsourkas, A. Firefly luciferase and RLuc8 exhibit differential sensitivity to oxidative stress in apoptotic cells. *PLoS One* **6**, e20073 (2011).
27. Fan, F. & Wood, K.V. Bioluminescent assays for high-throughput screening. *Assay Drug Dev. Technol.* **5**, 127–136 (2007).
28. Zhang, Y. *et al*. ABCG2/BCRP expression modulates D-Luciferin based bioluminescence imaging. *Cancer Res.* **67**, 9389–9397 (2007).
29. Maring, J.G., Piersma, H., van Dalen, A., Groen, H.J., Uges, D.R. & De Vries, E.G. Extensive hepatic replacement due to liver metastases has no effect on 5-fluorouracil pharmacokinetics. *Cancer Chemother. Pharmacol.* **51**, 167–173 (2003).
30. van Kuilenburg, A.B. *et al*. Evaluation of 5-fluorouracil pharmacokinetics in cancer patients with a c.1905 + 1G>A mutation in DPYD by means of a Bayesian limited sampling strategy. *Clin. Pharmacokinet.* **51**, 163–174 (2012).
31. Di Paolo, A. *et al*. 5-fluorouracil pharmacokinetics predicts disease-free survival in patients administered adjuvant chemotherapy for colorectal cancer. *Clin. Cancer Res.* **14**, 2749–2755 (2008).
32. Bocci, G. *et al*. Comparative pharmacokinetic analysis of 5-fluorouracil and its major metabolite 5-fluoro-5,6-dihydrouracil after conventional and reduced test dose in cancer patients. *Clin. Cancer Res.* **6**, 3032–3037 (2000).
33. Bergstrand, M. & Karlsson, M.O. Handling data below the limit of quantification in mixed effect models. *AAPS J.* **11**, 371–380 (2009).
34. Ahn, J.E., Karlsson, M.O., Dunne, A. & Ludden, T.M. Likelihood based approaches to handling data below the quantification limit using NONMEM VI. *J. Pharmacokinet. Pharmacodyn.* **35**, 401–421 (2008).
35. Yang, S. & Roger, J. Evaluations of Bayesian and maximum likelihood methods in PK models with below-quantification-limit data. *Pharm. Stat.* **9**, 313–330 (2010).
36. Keizer, R.J. *et al*. Incorporation of concentration data below the limit of quantification in population pharmacokinetic analyses. *Pharmacol. Res. Perspect.* **3**, e00131 (2015).

Supplementary information accompanies this paper on the *CPT: Pharmacometrics & Systems Pharmacology* website (http://www.wileyonlinelibrary.com/psp4)